

QUASIPERIODIC RESPONSE TO PARAMETRIC EXCITATIONS

J. M. LOPEZ* AND F. MARQUES†

Abstract. Parametric excitations are capable of stabilizing an unstable state, but they can also destabilize modes that are otherwise stable. Resonances come into play when the periodically forced base state undergoes a Hopf bifurcation from a limit cycle to a torus. A Floquet analysis of the basic state will identify such an event, but in order to characterize the resonances, one requires precise knowledge of the frequencies of the resultant quasiperiodic state. However, the Floquet analysis only returns the angle at which one of the pair of complex-conjugate eigenvalues cross the unit disk, modulo 2π . This angle is related in a non-trivial way to the new frequency resulting from the bifurcation. Here, we first present a technique to unambiguously determine the frequencies of the solutions following such a Hopf bifurcation, using only results from Floquet theory and discrete dynamical systems. We apply this technique to a periodically forced system susceptible to centrifugal instabilities and identify the conditions under which the system resonates, leading to resonance horns emerging from the Hopf bifurcation curves, and also identify locations of high codimension degenerate bifurcations resulting from space-time resonances.

Key words. Floquet theory, parametric excitation, quasiperiodic flow, Arnold's tongues, resonance horns.

1. Introduction to parametric excitations. The usual discussion of parametric excitations is in terms of systems where the governing equations are reduced to systems of Mathieu-type equations (Mathieu [21]). These reductions are strictly only possible in systems whose natural frequencies are fixed by external constraints. A typical example is Faraday waves (Faraday [9]), surface waves due to a harmonic oscillation of a container of fluid in the direction parallel to gravity. In ideal fluids of infinite extent and subjected to small amplitude oscillations, this excitation of the free surface is described by the Mathieu equation

$$\ddot{\eta} + (\Omega^2 + a \sin \omega t) \eta = 0, \quad (1.1)$$

where Ω is the natural frequency of surface waves in the unmodulated system, a and ω are the amplitude and frequency of the vertical oscillations of the container, and η is the vertical displacement of the free surface from its flat, mean position. This equation of Mathieu [21] has been studied extensively (see for example Jordan & Smith [15]). A simple mechanical system where it arises is in characterizing the motion of a simple pendulum subjected to a vertical oscillation of its pivot. This equation has provided

*Department of Mathematics, Arizona State University, Tempe AZ 85287-1804, USA. The work of the first author was supported in part by NSF grants DMS-9512483 and DMS-9706951.

†Departament de Física Aplicada, Universitat Politècnica de Catalunya, Jordi Girona Salgado s/n, Mòdul B4 Campus Nord, 08034 Barcelona, Spain. The work of the second author was supported in part by DGICYT grant PB94-1209.

the starting point for the study of parametric resonance. It is significant to note that the first reported observation of parametric resonance was by Faraday [9] in a hydrodynamic system and has since led to many important implications in many branches of engineering and physics. Examples of parametric resonance include the response of mechanical and elastic systems to time-varying loads. Parametric resonance due to even very small but finite vibrational loading can stabilize an unstable system, or destabilize a stable system, depending on particular characteristics of the system.

For systems that are governed by Mathieu-type equations (including linear damping terms), their response to parametric excitations can be expected to be either synchronous with the applied periodic forcing, or to have a subharmonic response (Davis & Rosenblat [8]). This means that when the trivial solution, i.e. the fixed point $\eta = 0$ in (1.1), loses stability, the bifurcating solution is either T -periodic (synchronous) or $2T$ -periodic (subharmonic), where $T = 2\pi/\omega$ is the period of the applied forcing.

Hydrodynamic systems in which parametric resonance has been identified and studied are typically characterized by their ability to support waves in the absence of external modulations (e.g. see Miles & Henderson [23]), and these are waves in the classic sense, i.e. surface waves, gravity waves, Rossby waves, etc. Many such hydrodynamic systems have been studied in certain distinguished limits (e.g. Benjamin & Ursell [4]; Gershuni & Zhukhovitskii [11]; Kelly [18]; Gresho & Sani [12]; Craik & Allen [7]), where the governing equations reduce to either a Hill's or (damped) Mathieu's equation. Not all hydrodynamic systems of interest reduce to these simple forms, but they still may be susceptible to parametric excitation. In general, the governing equations for the departures from the unforced state reduce to a form

$$\dot{\mathbf{x}} = (\mathbf{A} + \mathbf{B} \sin \omega t) \mathbf{x} + \mathbf{f}(\mathbf{x}), \quad (1.2)$$

where $\mathbf{f}(\mathbf{x})$ contains all the nonlinear terms. In general, (1.2) cannot be reduced to a system of (damped) Mathieu equations, and the response to parametric excitation can be more complicated than either synchronous or subharmonic.

An important difference between the stability of systems governed by Mathieu's equation and general systems is that in the former case the base state is a fixed point independent of the amplitude and frequency of the external forcing, whereas in more general systems, the base state is a periodic orbit that depends on the forcing parameters, usually with the same frequency as that of the forcing. In the classical Faraday experiment, for example, the basic state of the forced system is a rigid body motion and is at rest in the frame of reference of the container; the base state in this reference frame is unaware of the forcing. In general, there is no such reference frame when only some of the boundary conditions change due to the parametric excitation. So, in general, the basic state is also a function

of the amplitude and frequency of the forcing, and the base state is periodic with the period of the forcing.

The stability of the basic state of (1.2) is determined by applying classical Floquet theory (e.g. Joseph [16]; Guckenheimer & Holmes [13]) and numerical integration. The fundamental matrix is the solution of the system

$$\dot{\mathbf{X}} = \mathbf{M}(t)\mathbf{X}, \quad \mathbf{X}(0) = \mathbf{I}, \quad (1.3)$$

where \mathbf{I} is the identity matrix and $\mathbf{M}(t) = \mathbf{A} + \mathbf{B} \sin \omega t$. Integrating over a complete period $T = 2\pi/\omega$, one obtains the monodromy matrix of the system, $\mathbf{X}(T)$, whose eigenvalues γ_j , $j = 1, 2, \dots, N$, called Floquet multipliers, control the growth rate of the perturbations (N is the size of the discretized system).

From a dynamical systems point of view, integration over one period is equivalent to considering the Poincaré map over a complete period. Therefore, we move from the analysis of a periodic ODE, to the analysis of an autonomous map. The base state of (1.2) is a fixed point of the map. The eigenvalues of the monodromy matrix are the eigenvalues of the linearized Poincaré map in the neighborhood of the fixed point. If all the eigenvalues have moduli less than one, all the perturbations of the basic state go to zero, and the basic state is asymptotically stable (an attractor). The basic flow loses stability when at least one eigenvalue of the monodromy matrix crosses the unit circle. There are three different generic cases to be considered. If the critical eigenvalue crosses at $+1$ (a fold bifurcation), the bifurcated state is a fixed point of the map, corresponding to a periodic orbit of the original ODE with the same frequency as that of the forcing. The bifurcation is said to be synchronous and no new frequency is introduced. If the critical eigenvalue crosses at -1 , then we have a period doubling bifurcation where the fixed point becomes a period-2 fixed point of the map, corresponding to a periodic orbit of the original ODE with a frequency half of the forcing frequency, the so-called subharmonic case. For the Mathieu equation (with or without damping) these are the only possibilities when the basic state bifurcates (see Davis & Rosenblat [8]; Jordan & Smith [15]).

The third generic case corresponds to a loss of stability due to a pair of complex-conjugate eigenvalues crossing the unit circle not at ± 1 . Then, an attracting invariant circle emerges from the fixed point of the map. It is a Hopf bifurcation for maps, called a Naimark–Sacker bifurcation (see Arnold [2], Kuznetsov [19] for details). The periodic orbit of the original ODE is now surrounded by an invariant torus. On this torus, the solution of the system has two frequencies. One of the frequencies is the forcing frequency (the frequency of the basic state, ω), which survives the bifurcation. The other bifurcating frequency, denoted ω_s , is associated with the phase (angle of crossing) of the complex-conjugate critical eigenvalues of moduli one, $\gamma_{1,2} = e^{\pm i\phi}$, $\phi = 2\pi\omega_s/\omega$. General hydrodynamic systems of the form (1.2)

can experience such a bifurcation. It is this case that is of primary interest here.

Notice that for the angle ϕ in $\gamma_{1,2} = e^{\pm i\phi}$, its absolute value is unique only modulo 2π . Therefore, the definition of the bifurcating frequency as $\omega_s = \omega\phi/2\pi$ is ambiguous. However, this ambiguity can be removed for continuous systems. Near the bifurcation, the Poincaré map \mathbf{P} is a diffeomorphism of the invariant bifurcating circle. For such a diffeomorphism the *rotation number* is defined as the average angle by which the map rotates the invariant circle; the definition involves a limit for $n \rightarrow \infty$ of the iterates \mathbf{P}^n for nonlinear systems, but for linear systems \mathbf{P} is a rigid rotation whose angle equals the rotation number. This number is unique mod(2π), removing the previous sign ambiguity. When \mathbf{P} is the period-1 map of a continuous system such as (1.2), then the remaining ambiguity associated with the mod(2π) can also be removed by following the continuous system during a whole period and *continuously* monitoring the angle rotated, or using continuation methods based on the continuity of the rotation number with respect to the parameters of the problem. This unambiguously defined angle, a generalization of the rotation number for continuous systems, is called the *self-rotation number* ϕ_{sr} . All the pertinent definitions and proofs can be found in Peckham [24]. The bifurcating eigenvalues at criticality are $\gamma_{1,2} = e^{\pm i\phi_{sr}}$. We finally *define* the bifurcating frequency as $\omega_s = \omega\phi_{sr}/2\pi$. In the following, we will refer to the self-rotation number simply as ϕ .

The dynamics of solutions on the invariant torus depend critically on the self-rotation number. If $\omega_s/\omega = \phi/2\pi$ is irrational, then all the trajectories are dense on the torus. If ω_s/ω is rational, then $\gamma_{1,2}^q = 1$ for some integer q , and there are periodic orbits on the torus. In this case, there is resonance; for $q \leq 4$ it is a *strong resonance* and for $q \geq 5$ it is a *soft resonance*.

The Naimark–Sacker bifurcation is in fact a codimension–2 bifurcation. It is convenient to consider the bifurcation as taking place on a two-parameter plane. On this plane there is a curve (the Hopf or Naimark–Sacker bifurcation curve), consisting of the locus of points where the Floquet multipliers are on the unit circle. On one side of the curve, there is a stable limit cycle and on the other side (supercritical) there is a stable invariant torus. Along the bifurcation curve, the ratio ω_s/ω is continuous with variations in the two parameters. If this ratio is rational, $\omega_s/\omega = p/q$, p and q integers, there is a p/q -resonance. As the parameters are varied supercritically away from these p/q -resonance points on the Hopf curve, there is a finite region of parameter space associated with each resonance point in which the dynamics are locked into the p/q -resonance. These regions have the appearance of horns, with their tips located on the Hopf curve at the p/q -resonance points, and are referred to as resonance horns or Arnold’s tongues.

For small supercritical distances from the Hopf curve, Arnold [2] and

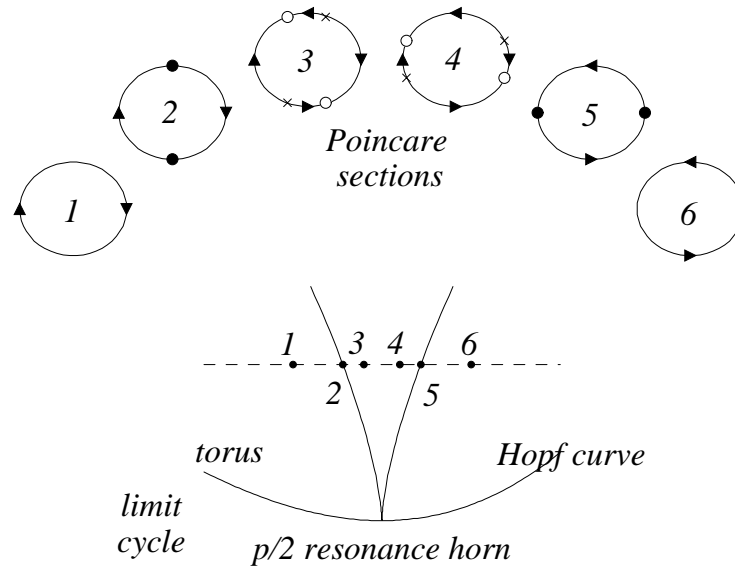


FIG. 1. Dynamics on the torus in the neighborhood of a $p/2$ -resonance horn. The Poincaré sections 1–6 of the torus correspond to the dashed supercritical trajectory through the horn. On these sections, \bullet is a saddle-node bifurcation point, \circ is a sink, and \times is a saddle. The torus attracts nearby orbits.

Kuznetsov [19] give a description of the dynamics associated with the resonance horns for maps. Gambaudo [10] gives the corresponding description for ODE systems. Figure 1 is a schematic of the crossing of a $p/2$ -resonance horn. Even though p/q -resonance horns with $q \leq 4$ are special, we have drawn the $q = 2$ case to keep the figure simple, but the following description is for general q . If one considers the dynamics as a p/q -resonance horn is traversed, outside the horn there are no periodic points with rotation number p/q . At the boundary of the horn, q saddle-nodes appear on the invariant circle corresponding to the Poincaré section of the torus. In the interior of the horn, the saddle-nodes bifurcate forming q saddle-sink pairs, which move apart as we proceed deeper into the horn. As the other boundary is approached, these points form different saddle-sink pairs that bifurcate to saddle-nodes on the boundary and vanish on crossing the boundary of the horn. We expect to have similar behavior in PDE systems, but the PDE case has not been analyzed to our knowledge.

For strong resonances ($q \leq 4$), the torus is expected to break-up, for example, due to homoclinic/heteroclinic dynamics, even close to the Hopf curve (Gambaudo [10], Kuznetsov [19]). For further details and examples of the behavior associated with resonance horns (in ODE systems), see

Aronson *et al.* [3], McKarnin *et al.* [22], Peckham *et al.* [25].

In Mathieu's equation (1.1), the natural frequency, $\omega_s = \Omega$, is known *a priori* and is independent of the forcing. In a generic ODE, and in our PDE problems, the second frequency following the Hopf bifurcation, ω_s , is not known *a priori*, and in general depends on the forcing in a nonlinear and possibly discontinuous fashion. In order to determine the self-rotation number and identify the location of the resonance points on the Hopf curve, one must determine the imaginary parts of the Floquet exponents unambiguously, as these give ω_s . Floquet analysis does not determine the imaginary parts of the Floquet exponents unambiguously and so when a quasiperiodic state results, the question arises as to how to determine its frequencies.

2. Correcting the phase and extracting the frequency. From Floquet theory, a linear problem with periodic coefficients like (1.3) has a set of fundamental solutions at criticality of the form

$$\mathbf{x}(t) = \mathbf{x}_p(t)e^{\pm i\omega_s t}, \quad (2.1)$$

with $\mathbf{x}_p(t)$ periodic, i.e. $\mathbf{x}_p(t+T) = \mathbf{x}_p(t)$, where $T = 2\pi/\omega$ is the period of the applied forcing. Therefore, the critical Floquet multipliers are $\gamma_{1,2} = e^{\pm i\omega_s T}$. However, the Floquet analysis does not give the self-rotation number $\phi = \omega_s T$, but rather an angle $\tilde{\phi} \in [0, \pi]$. In general, the phase of a complex conjugate number is an angle in $[0, 2\pi)$, but we have a pair of complex conjugate eigenvalues, giving two angles ϕ and $2\pi - \phi$ (modulo 2π). For definiteness, we select the smallest in $[0, \pi]$. The relationship between $\tilde{\phi}$ and ϕ is

$$\phi = 2l\pi \pm \tilde{\phi}, \quad (2.2)$$

where the sign and the integer multiple l are undetermined. So the question arises as to how to unambiguously determine ω_s . We have developed a method to determine the self-rotation number from computations over one period of the base state at various points in parameter space that uses the continuity of the eigenvalues of the system and homotopy considerations, based on the work of Peckham [24].

Let ϕ be the self-rotation number, $\omega_s = \phi/T$, and $\tilde{\omega} = \tilde{\phi}/T$. We first establish the relationship between the self-rotation number, ϕ , and the phase given by the Floquet analysis, $\tilde{\phi}$. When ϕ lies in the interval $[2l\pi, (2l+1)\pi]$, the Floquet analysis gives $\tilde{\phi} = \phi - 2l\pi$; and when $\phi \in [(2l+1)\pi, (2l+2)\pi]$, the Floquet analysis gives $\tilde{\phi} = (2l+2)\pi - \phi$. Incorporating both cases into a single expression, then for $\phi \in [m\pi, (m+1)\pi]$,

$$\phi = \left(m + \frac{1}{2}\right)\pi + (-1)^m \left(\tilde{\phi} - \frac{\pi}{2}\right). \quad (2.3)$$

For an isolated point in parameter space, we do not know ϕ and m is undetermined. However, if we know the value of m for a particular state of the

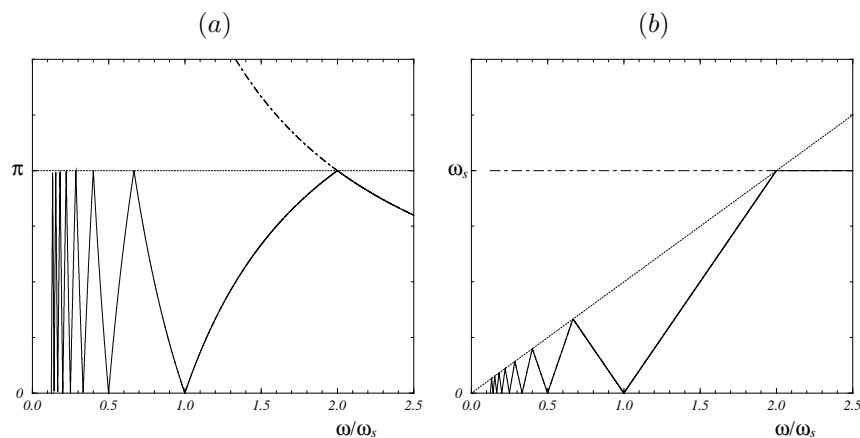


FIG. 2. (a) Phase of the bifurcating solution vs. ω/ω_s ; dot-dash line: self-rotation number $\phi = 2\pi\omega_s/\omega$; solid line: phase from the analysis ϕ ; (b) frequency of the bifurcating solution vs. ω/ω_s ; dot-dash line: true frequency ω_s ; solid line: frequency from the analysis $\tilde{\omega}$; and dotted line: $\omega_s = 0.5\omega$.

system, corresponding to a certain combination of parameter values, we can determine the value of m for any other state continuously connected with the known particular state. In fact, m remains constant as the parameters are varied continuously unless $\tilde{\phi}$ goes through zero or π . In these cases, from (2.3),

$$\tilde{\phi} \rightarrow 0 \Rightarrow m \rightarrow m - (-1)^m, \quad \text{and} \quad \tilde{\phi} \rightarrow \pi \Rightarrow m \rightarrow m + (-1)^m. \quad (2.4)$$

The deduction is as follows. When $\tilde{\phi} \rightarrow 0$ for a given value of m (i.e. $\phi \in [m\pi, (m+1)\pi]$), (2.3) gives $\phi \rightarrow (m + (1 - (-1)^m)/2)\pi$. For m even, $\phi \rightarrow m\pi$, and therefore ϕ moves to the interval $[(m-1)\pi, m\pi]$, and hence m decreases by one. For m odd, $\phi \rightarrow (m+1)\pi$, and therefore ϕ moves to the interval $[(m+1)\pi, (m+2)\pi]$, and so m increases by one. An analogous argument applies when $\tilde{\phi} \rightarrow \pi$.

In order to apply (2.4) we need to know the value of m for some state of the system. The problem is that we do not know what m is for any isolated case. In general however, in the limit that the forcing amplitude goes to zero, the second bifurcation frequency ω_s asymptotes to the natural frequency of the unforced system, and in the limit of large forcing frequency, one obtains $\omega_s \ll \omega$ so that $\phi = 2\pi\omega_s/\omega < \pi$ and hence $m = 0$. For any particular problem, there may be other means of determining m in some part of parameter space by taking appropriate limits.

As an example of this method of determining the frequency ω_s from $\tilde{\phi}$, we consider the idealized case in which the bifurcating frequency, ω_s , is independent of the forcing frequency ω . The self-rotation number and the

bifurcating frequency are related by

$$\frac{\phi\omega}{2\pi} = \omega_s = \text{constant}, \quad (2.5)$$

so we have $\phi = (2\pi\omega_s)/\omega$, i.e. the self-rotation number is inversely proportional to the frequency of the basic flow (the forcing frequency ω). Figure 2a shows this relationship as a dot-dash line, along with the phase $\tilde{\phi}$ that results from the Floquet analysis as a solid line. The values of ω where $\tilde{\phi} = 0$ correspond to the locations of the tips of resonance horns, i.e. where the bifurcating frequency ω_s is an integer multiple of the forcing frequency ω . The values of ω where $\tilde{\phi} = \pi$ are not special and correspond to subharmonic responses, i.e. the bifurcating frequency is an odd multiple of $\omega/2$. Apart from these two classes of forcing frequencies, the system responds quasiperiodically. In the simple case that ω_s is independent of ω , it is straightforward to determine ω_s from $\tilde{\omega} = \tilde{\phi}/T$ using (2.4). This is shown in Figure 2(b).

In general, and in particular as the amplitude of the forcing is increased, ω_s will be a function of ω . The relationship $\tilde{\omega} = \tilde{\phi}/T$ still applies and (2.3) and (2.4) can still be used, but now we lack *a priori* knowledge of exactly where the synchronous and subharmonic points are, i.e. the value of m at any given ω . This is not a serious limitation for ω corresponding to small m , but as $\omega \rightarrow 0$ it very quickly becomes exceedingly difficult to determine the corresponding value of m .

There are further complications that arise when there are catastrophic jumps in the spatial structure of the solution as either the frequency or amplitude of the applied forcing is varied smoothly. We have assumed that the phases ϕ and $\tilde{\phi}$ are continuous functions of the parameters of the system, and in particular of ω . This is true for systems of finite dimension, but for infinite dimensional systems, the issue is more difficult (Kato [17]). Nevertheless, our analysis refers to the numerically computed phases obtained from the discretization of the system, which is always of finite dimension. So we will consider that the phases are continuous functions of the parameters. Only an additional problem remains: for particular parameter values two different pairs of complex-conjugate eigenvalues can simultaneously cross the unit circle. In these cases, the most dangerous eigenvalue can change from one complex-conjugate pair to another in a neighborhood of the critical parameter values. Then, although the phases on both eigenvalue branches are continuous, the phase of the critical state is discontinuous because we must switch branches when following the most dangerous eigenvalue. This behavior may arise when more than one parameter is varied and higher codimension points are encountered where more than one mode become critical. In the following section we illustrate cases where this problem arises and how our technique may still be used to robustly and unambiguously determine the frequencies of these quasiperiodic flows.

3. Parametrically forced Taylor–Couette flow. In Hu & Kelly [14] and Marques & Lopez [20], the stability of such a hydrodynamic system was investigated using Floquet theory. The system in question is the flow between two co-axial cylinders, the outer one being stationary and the inner one rotating at some fixed rate (the usual Taylor–Couette flow), and the inner cylinder is also subjected to a harmonic oscillation in the axial direction (see figure 3). This system has also been investigated experimentally by Weisberg, Kevrekidis & Smits [27]. The system is governed by a number of nondimensional parameters. Dimensionally, the inner cylinder oscillates in the axial direction with velocity $U \sin \Omega t$ and rotates at constant angular velocity Ω_i . Its radius is r_i and the radius of the outer stationary cylinder is r_o . The annular gap between the cylinders is $d = r_o - r_i$. These parameters are combined to give the following nondimensional governing parameters:

$$\begin{aligned} \text{the radius ratio} & e = r_i/r_o, \\ \text{the Couette flow Reynolds number} & Re_i = dr_i\Omega_i/\nu, \\ \text{the axial Reynolds number} & Re_a = dU/\nu, \\ \text{the nondimensional frequency} & \omega = d^2\Omega/\nu, \end{aligned}$$

where ν is the kinematic viscosity of the fluid. The basic flow is time-periodic and synchronous with the forcing, but it is independent of the azimuthal and axial coordinates.

The system is governed by the Navier–Stokes equations, which are reduced to a system of ODE by using a Galerkin expansion based on Chebyshev polynomials. The stability analysis of the time-periodic basic state is then reduced to the determination of the growth rates of the solutions of a linear system of the form:

$$G\dot{\mathbf{x}} = H(t)\mathbf{x} = (A + B \sin \omega t + C \cos \omega t)\mathbf{x}. \quad (3.1)$$

The entries in the matrices G and H are given in the appendix of Marques & Lopez. H is periodic, of period $2\pi/\omega$, where ω is the frequency of the axial oscillations of the inner cylinder, and G is time-independent and positive definite. Since G is invertible, (3.1) can be written in the form (1.3). The axial and azimuthal wave numbers of the bifurcating solutions are k and n , respectively.

The Navier–Stokes equations governing this problem are invariant under translations (τ) along and rotations (R) around the common axis of the cylinders. Moreover, there exists an additional discrete symmetry (S) involving the time and the axial coordinate; it is a reflection about the plane orthogonal to the axis with a simultaneous time-translation of a half period. The symmetry S satisfies $S^2 = I$, and the symmetry group of our problem is $SO(2) \times SO(2) \times Z_2$. The presence of these symmetries has many consequences on the dynamics and the bifurcations this system can experience. Chossat & Iooss [5] give details specific to the classical

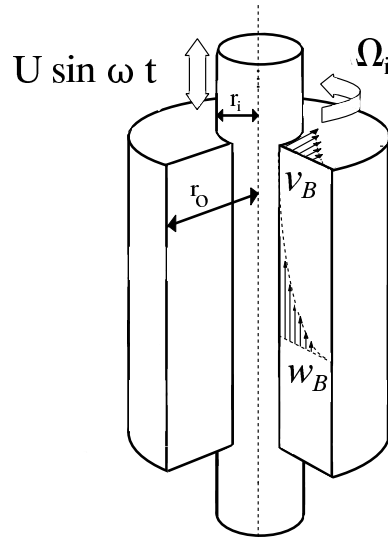


FIG. 3. Schematic of Taylor–Couette flow with axial oscillations of the inner cylinder.

Taylor–Couette problem. In our case, due to the symmetry S , we need only consider the $n \geq 0, k \geq 0$ cases.

In the Taylor–Couette flow with axial oscillations of the inner cylinder, the basic state consists of circular Couette flow with a superimposed annular Stokes flow. It is independent of the axial and azimuthal directions, and time-periodic with the period of the forcing; an analytic description of the basic flow is derived in Marques & Lopez [20]. Over an extensive range of parameter space, the primary bifurcation is to an axisymmetric state that is periodic in the axial direction and time, with the same temporal period as the forcing (Weisberg *et al.* [27]; Marques & Lopez [20]). Due to the symmetries of the system, the bifurcation is not the generic fold or saddle–node bifurcation, but a pitchfork for periodic orbits (Kuznetsov [19]). When the basic solution loses stability, two time-periodic solutions resembling Taylor vortices appear; the symmetry S changes one to the other.

The analysis of Marques & Lopez [20] however, showed that in narrow windows of parameter space, where interaction and competition between different axial modes occurs, the primary bifurcation is to a state that is periodic in both the axial and the azimuthal directions, and temporally has the forcing frequency as well as a new frequency ω_s , so that the dynamics are on a torus. These regions in parameter space are pockets of spatio-

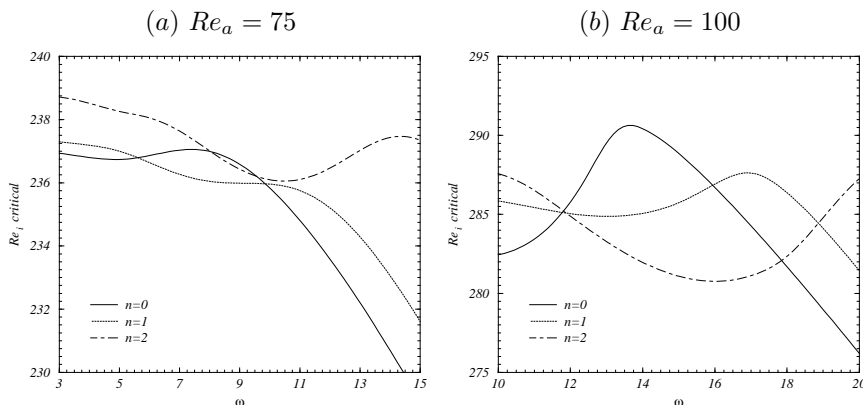


FIG. 4. Critical Re_i versus ω in for (a) $Re_a = 75$ and (b) $Re_a = 100$, and various azimuthal modes n as indicated.

temporal complexity. Part of their figure 10 is reproduced here as figure 4, showing examples for the radius ratio $e = 0.905$ case. When $Re_a = 75$ there is a range of ω over which the azimuthal mode $n = 1$ is most dangerous and for $Re_a = 100$, the $n = 2$ mode is most dangerous. Normally, in the unforced Taylor–Couette flow, these azimuthal modes are interpreted as either single ($n = 1$) or double ($n = 2$) spirals, but here, they can manifest themselves as tilted, wobbling, and deforming Taylor cells, due to the interaction with the axial and temporal periodicities. Such tilted cells were noted in the experiments of Weisberg [26] within the same parameter range, but were not investigated in detail in that study. Hu & Kelly [14] only considered the axisymmetric modes ($n = 0$) for this flow, but did consider non-axisymmetric modes in the Taylor–Couette flow with an imposed time-periodic axial pressure gradient. In the range of parameters they considered, the axisymmetric mode was most dangerous.

We shall begin by analyzing the $Re_a = 75$ case where the amplitude of the periodic forcing is large enough that over a range of the forcing frequency the bifurcation is to a torus and the resulting second frequency, ω_s , varies with the forcing frequency ω (as well as with the forcing amplitude Re_a). From figure 4a, we see that the axisymmetric mode $n = 0$ is the most dangerous (i.e. for a given Re_a , ω , and n , the lowest value of Re_i over the range of axial wave numbers k at which a pair of Floquet multipliers first cross the unit circle), except in the range $5.6 < \omega < 9.8$, where the azimuthal mode $n = 1$ is most dangerous. The higher azimuthal modes ($n \geq 2$) have larger critical Re_i for any given ω at this forcing amplitude ($Re_a = 75$), and so would not normally be observed in any physical realization of the flow.

A limit in which it is clear how to extract ω_s from $\tilde{\phi}$ is in the limit

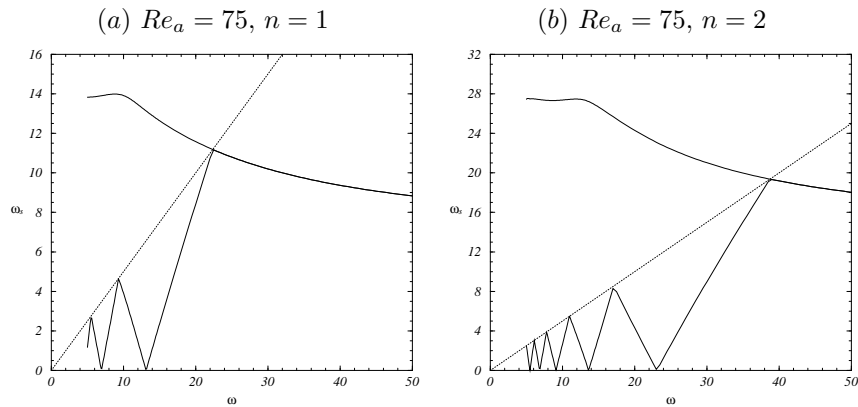


FIG. 5. Frequency of the bifurcating solution $\omega_s(\omega)$ (together with $\tilde{\omega}$ from which $\omega_s(\omega)$ was reconstructed, shown under the dotted line) when $Re_a = 75$ for azimuthal modes (a) $n = 1$ and (b) $n = 2$.

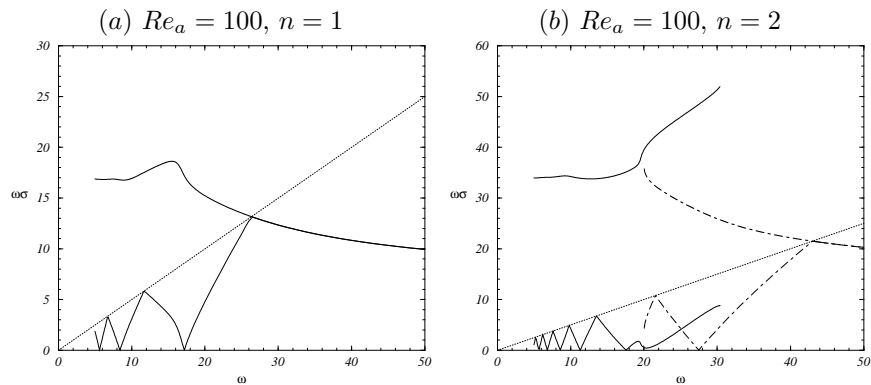


FIG. 6. Frequency of the bifurcating solution $\omega_s(\omega)$ (together with $\tilde{\omega}$ from which $\omega_s(\omega)$ was reconstructed, shown under the dotted line) when $Re_a = 100$ for azimuthal modes (a) $n = 1$ and (b) $n = 2$; note the two branches for $n = 2$.

of very weak forcing ($Re_a \rightarrow 0$), as in this limit ω_s is independent of the forcing (Re_a and ω). By dividing $\tilde{\phi}$ from the Floquet analysis of a weakly forced system by the forcing frequency ω , and adjusting the sign and adding the multiples of 2π so that it matches the natural frequency of the unforced ($Re_a = 0$) system, one can then determine ω_s . This is the technique employed by Hu & Kelly [14]. However, it is not applicable as Re_a becomes larger, and in the present example with $Re_a = 75$ it is ambiguous. At high Re_a , ω_s may be some multiple of 2π different from the natural frequency of the unforced flow. Another limit in which it is possible to determine ω_s unambiguously from $\tilde{\phi}$ is $\omega \rightarrow \infty$. For ω large enough, the

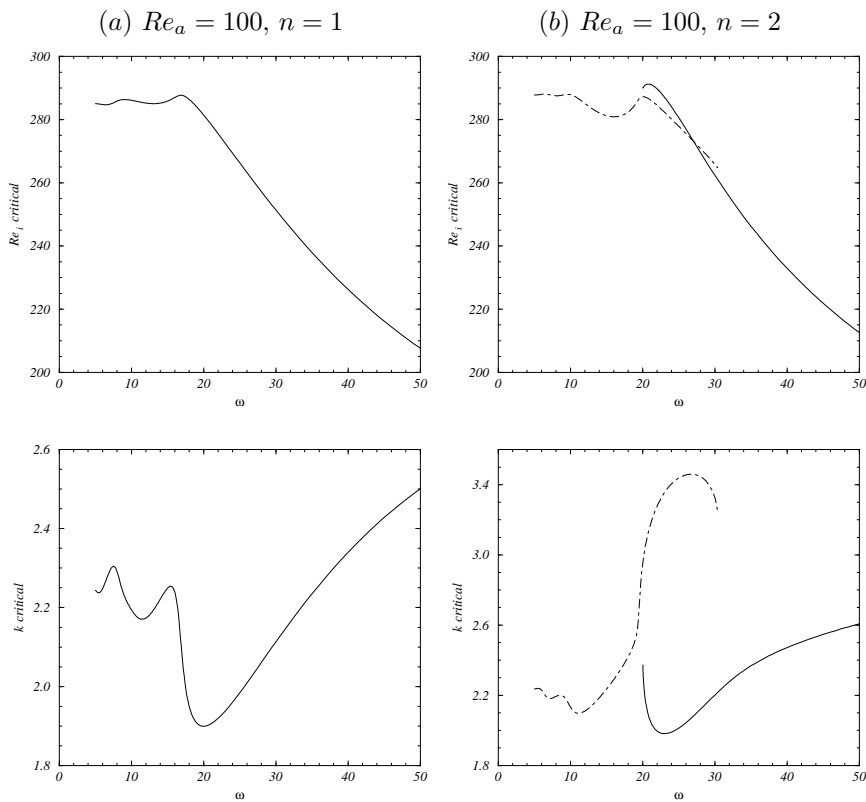


FIG. 7. Critical Re_i and k versus ω for $Re_a = 100$ and azimuthal modes (a) $n = 1$ and (b) $n = 2$.

effect of the external forcing on the flow goes to zero, because it is confined to the Stokes boundary layer of thickness $\sqrt{2/\omega}$ (Marques & Lopez [20]). Therefore ω_s remains constant, and from (2.2), $\phi = 2\pi\omega_s/\omega \rightarrow 0$. Then, $\phi \in [0, \pi]$ and $m = 0$. In figure 5a, we plot both $\tilde{\omega}$ and ω_s obtained by determining the self-rotation number as in §2. It should be compared with figure 2b, which corresponds to the ideal cases where $\omega_s = \text{constant}$.

For larger Re , the dependence of ω_s on ω becomes increasingly more nonlinear. For the $n = 1$ case at $Re_a = 100$, the quasiperiodic response when ω is in the neighborhood of 15 is particularly nonlinear (see figure 6a). However, the locus of primary Hopf bifurcation points is continuous in ω , and using the techniques of §2, we are still able to determine the self-rotation number, and hence the second bifurcating frequency ω_s . Note that the critical Re_i and k change dramatically with both Re_a and ω (see figure 7). From figure 4b, for $Re_a = 100$, the $n = 0$ mode is the most dangerous except in the range $11.91 < \omega < 17.84$, where the $n = 2$ mode is

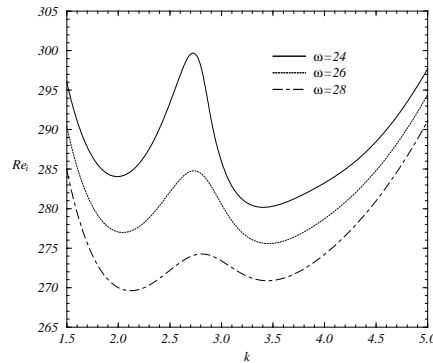


FIG. 8. *Stability boundaries in (Re_i, k) space for $Re_a = 100$, azimuthal mode $n = 2$, and ω as indicated.*

the most dangerous, and for a very small range $11.74 < \omega < 11.91$, $n = 1$ dominates. For lower Re_a , the window of non-axisymmetric response is shared more evenly between the $n = 1$ and $n = 2$ modes, and as Re_a is reduced further $n = 1$ dominates, as described above.

The determination of the frequency ω_s in the $n = 2$ case is much more complicated. Here, the locus of primary Hopf bifurcation points is not continuous in ω for fixed Re_a . Instead, we find a range $20.045 < \omega < 30.380$ over which the stability curves Re_i vs. k have two minima (figure 8), each corresponding to distinct branches (i.e. loci of local minima in Re_i for variable ω and fixed Re_a) of bifurcating solutions. There is a large difference in the axial wavelengths associated with these two branches. Over the range of ω where the two $n = 2$ solutions co-exist, the $n = 0$ solution is the most dangerous and hence the $n = 2$ solutions would not be physically realized. The two branches, where they exist, are continuous, branch 1 for $\omega > 20.045$ and branch 2 for $\omega < 30.380$. From figure 4b we see that over the range $11.8 < \omega < 17.8$, branch 2 is physically observable, and it would be of great interest to be able to predict the frequencies associated with this quasiperiodic flow.

The determination of ω_s on branch 1 is straightforward. Since the branch extends beyond $\omega > 2\omega_s$, we can directly apply the technique from §2, starting from a suitably large ω where $m = 0$ and detect the synchronous ($\tilde{\phi} = 0$) and subharmonic ($\tilde{\phi} = \pi$) points as ω is reduced in order to determine m . Such a straightforward application is not possible for branch 2 as, for fixed $Re_a = 100$, it ceases to exist for some $\omega < 2\omega_s$, so we do not have a simple method to determine m . However, branch 2 is continuous, as illustrated by the curves of critical Re_i and k in figure 7b, and so it is reasonable to expect (Kato [17]) that ω_s will also be continuous on branch 2.

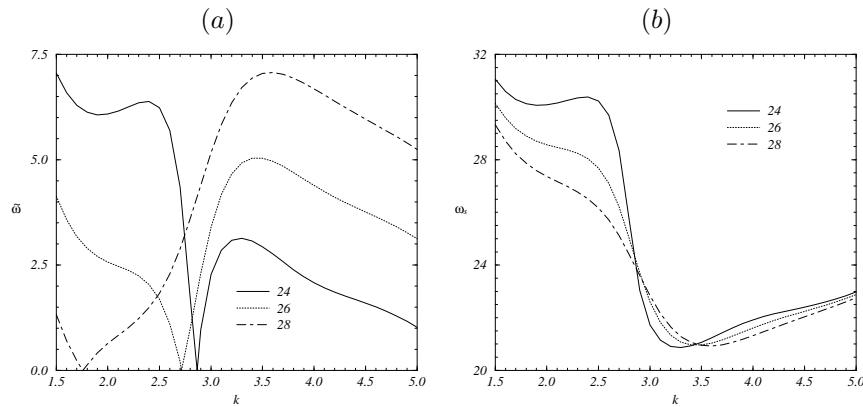


FIG. 9. (a) Frequency from the Floquet analysis $\tilde{\omega}$ and (b) the corresponding ω_s , versus axial wavenumber k , for $Re_a = 100$, $n = 2$, and forcing frequency ω as indicated

We shall use the continuity of eigenvalues from finite dimension systems theory (Kato [17]) in order to determine ω_s corresponding to branch 2, which does not extend to $\omega \rightarrow \infty$. The point is that the eigenvalues (in this case, ω_s) are not only continuous functions of the forcing frequency ω , but of *all* parameters governing the flow, and in particular of the axial wavenumber k . The locus of points where the eigenvalues cross the unit disk in the multi-dimensional parameter space governing the system is a continuous manifold, and this manifold may have folds so that a particular cut through the fold with all parameters fixed except for one of them, may have a discontinuity in the eigenvalue as a function of that parameter. However, with a suitable variation of the other parameters, a continuous connection between any two points on the manifold can be established. So, when we talk about branches, we mean particular cuts through this manifold on which the eigenvalues are continuous functions of the varying parameter.

In order to determine ω_s for branch 2, as illustrated in figure 6b, we have selected an ω where both branches co-exist, and where we know the value of m corresponding to branch 1 (e.g. $\omega = 28$, corresponding to the dot-dash line in figure 8). We start from the minimum on the Re_i versus k curve corresponding to branch 1 ($k \approx 2.2$), where from figure 6b we know that $m = 1$. Then we vary k at the fixed $\omega = 28$ value, keeping track of when $\tilde{\phi} \rightarrow 0$ or π to increment m , until we reach the other minimum, corresponding to the branch 2 solution ($k \approx 3.4$). Once this is done, we have the value of m on a particular point on branch 2, and by continuity with varying ω , the ω_s on the entire branch 2 can be determined in the manner described earlier. This determination is illustrated in figure 6b. Examples at other fixed ω values for varying k are shown in figure 9. These distinct

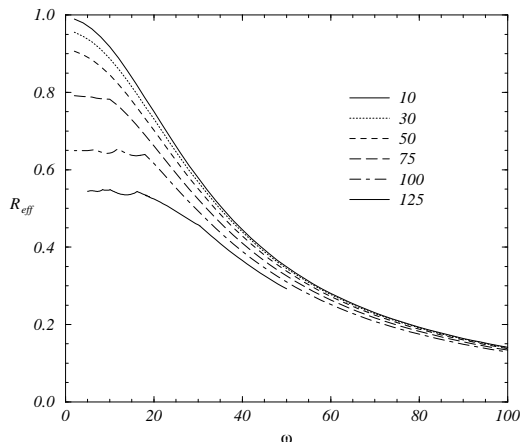


FIG. 10. Relative efficiency R_{eff} of the forcing amplitude Re_a (as indicated) in delaying the transition vs. forcing frequency ω .

determinations with varying k are consistent with the results shown in figure 6b, and give an additional check of the continuity-based technique.

4. Quasiperiodic windows and parametric resonance. We have seen from both theory (Hu & Kelly [14]; Marques & Lopez [20]) and experiment (Weisberg *et al.* [27]) that the parametric excitation of the Taylor–Couette flow is capable of stabilizing the centrifugal instability (i.e. the transition to axisymmetric Taylor cells) substantially, as measured by

$$R_{\text{eff}} = \frac{\mathcal{N} \left(\text{critical } Re_i \right) - \left(\text{critical } Re_i \text{ at zero forcing} \right)}{Re_a^2 \left(\text{critical } Re_i \text{ at zero forcing} \right)},$$

where \mathcal{N} is a normalization factor such that $R_{\text{eff}} \rightarrow 1$ when the forcing is most efficient in delaying the onset of instability in the basic flow to larger Re_i . This occurs at the double limit $\omega \rightarrow 0$ and $Re_a \rightarrow 0$. This ratio gives the degree of enhancement of the critical inner cylinder rotation rate relative to the unforced flow to the amplitude squared of the forcing (the critical Re_i at zero forcing is 134.94 for the flow geometry under consideration). In fact, R_{eff} is the ratio between the degree of stabilization obtained and the energy required (proportional to the forcing amplitude squared). Figure 10 shows R_{eff} as a function of the forcing frequency ω . There is a partial collapse of this relationship (as first noted by Hu & Kelly [14] at small forcing amplitudes), over a wide range of Re_a and particularly for small amplitude and large frequency of the forcing. To quadruple the degree of stabilization at a given frequency, one only needs to double the amplitude.

When the primary bifurcation is axisymmetric, it has always been

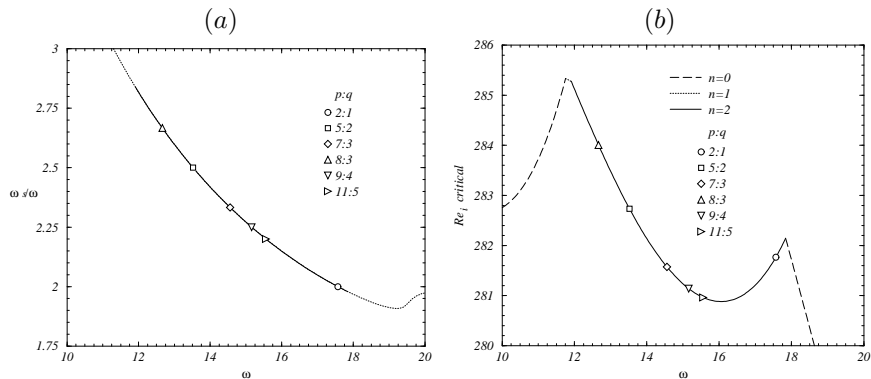


FIG. 11. (a) Response curves for $Re_a = 100$ and azimuthal modes n as indicated. The solid sections indicate the range of forcing frequency ω over which the corresponding mode is dominant (most dangerous). The symbols indicate the locations of strong resonance points; and (b) the corresponding excitation diagram.

observed (both experimentally and from the Floquet analysis) to be to another period-1 state, synchronous with the forcing. In the unforced Taylor–Couette flow, even though the primary bifurcation is to axisymmetric steady Taylor vortex flow, bifurcations also exist to non-axisymmetric time-periodic flows, with their own natural frequencies. For example, for $n = 1$ the natural frequency is 7.111 at the critical $Re_i = 135.59$, and for $n = 2$ it is 14.45 at the critical $Re_i = 137.60$. These natural frequencies vary slowly as Re_i changes from criticality (Antonijoan *et al.* [1]). These natural frequencies are the corresponding limits of ω_s as $Re_a \rightarrow 0$. Our observation is that while the axial oscillations of the inner cylinder stabilizes the axisymmetric mode, when the amplitude of the oscillations Re_a is large enough at frequencies ω close to the natural frequencies of the unforced system, then it also tends to destabilize the corresponding non-axisymmetric modes. In the geometry considered, for Re_a greater than about 68, we begin to observe primary bifurcations to non-axisymmetric modes.

The dramatic reduction in the efficiency R_{eff} observed in figure 10 for small ω and large Re_a comes into play as the non-axisymmetric modes become dominant. The dominance of these modes is a direct result of the parametric resonance exciting these spatio-temporal modes.

In order to characterize the resonances at play, we locate the strong resonance points on the Hopf curves. Figure 11a shows ω_s/ω vs. ω (the response curve) for $Re_a = 100$ and azimuthal mode $n = 2$ (the segment of this curve over which this mode is the most dangerous is indicated as a solid line). This curve was obtained from the Floquet analysis together with the phase correction technique of §2, and corresponds to the results in figures 4b and 6b. On the dominant (solid) part of the curve we locate the points of strong resonance, p/q with $q \leq 4$. It should be noted that the

solid curve is dense in soft resonance points ($q \geq 5$). Figure 11b is the corresponding critical Re_i vs. ω curve (the excitation diagram). For fixed $Re_a = 100$ and Re_i below this curve, the basic state is stable. When Re_i is increased above this curve with ω in the range where the response is quasiperiodic, all the complex resonant behavior described in the introduction is expected to appear. As one moves away supercritically from the Hopf curve in two-parameter space, complex dynamics including chaos and homoclinicity can be expected in the interior of the resonance horns, often quite close to the Hopf curve, and particularly for those corresponding to the strong resonances whose tips reside at the points indicated on the excitation diagram (figure 11b).

Other points close to which complexity can be expected are where the spatially dominant modes change. The multi-critical points, such as the switch from $n = 0$ to $n = 1$ at $\omega = 11.74$, $n = 1$ to $n = 2$ at $\omega = 11.91$, and $n = 2$ to $n = 0$ at $\omega = 12.84$ are where either two pairs of complex-conjugate eigenvalues or a real and a pair of c. c. eigenvalues simultaneously cross the unit disk. From these high codimension bifurcations, complexity can be expected directly (Chow *et al.* [6]). This spatial complexity comes about as the different azimuthal modes, each with different axial wavenumbers, compete to become dominant at these higher codimension points. This complexity is in addition to the temporal complexity discussed above in relation to the resonance horns. These competitions between spatial modes only come about here as a result of the temporal forcing; in the unforced system the primary bifurcation is to the $n = 0$ mode.

There are still further spatial complexities where modes with the same azimuthal wavenumber but different axial wave numbers compete, as illustrated in figure 8. In this example, there is a range of ω over which two $n = 2$ modes co-exist. Figure 10 for $Re_a = 125$ at $\omega = 30.41$ also shows this type of mode competition between two axisymmetric ($n = 0$) modes, with the new mode dominating at the lower ω values and also significantly reducing the efficiency R_{eff} of the dynamic forcing. In the unforced system, this does not occur; the marginal stability curve (Re_i vs. k) has a single minimum. The temporal forcing then, is seen to excite not only temporal resonances, but also spatial resonances.

Acknowledgment. The authors wish to express their thanks to I. Kevrekidis for his useful suggestions and discussions on resonance horns.

REFERENCES

- [1] ANTONIJOAN, J., MARQUES, F. & SANCHEZ, J. *Nonlinear spirals in the Taylor–Couette problem*. Phys. Fluids (1998), pp. 829–838.
- [2] ARNOLD, V. I. *Geometrical Methods in the Theory of Ordinary Differential Equations*, Springer–Verlag, 1988.
- [3] ARONSON, D. G., CHORY, M. A., HALL, G. R. & MCGEHEE, R. P. *Bifurcations from an invariant circle for two-parameter families of maps of the plane: a*

- computer-assisted study*. Commun. Math. Phys. **83** (1982), pp. 303–354.
- [4] BENJAMIN, T. B. & URSELL, F. *The stability of the plane free surface of a liquid in vertical periodic motion*. Proc. R. Soc. London A **225** (1954), pp. 505–515.
- [5] CHOSSAT, P. & IOOSS, G. *The Couette–Taylor Problem*, Springer–Verlag, 1994.
- [6] CHOW, S.-N., LI, C. & WANG, D. *Normal Forms and Bifurcations of Planar Vector Fields*, Cambridge University Press, 1994.
- [7] CRAIK, A. D. D. & ALLEN, H. R. *The stability of three-dimensional time-periodic flows with spatially uniform strain rates*. J. Fluid Mech. **234** (1992), pp. 613–627.
- [8] DAVIS, S. H. & ROSENBLAT S. *On bifurcating periodic solutions at low frequency*. Studies in Applied Mathematics **57** (1977), pp. 59–76.
- [9] FARADAY, M. *On a peculiar class of acoustical figures; and on certain forms assumed by groups of particles upon vibrating elastic surfaces*. Philos. Trans. R. Soc. Lond. **121** (1831), pp. 299–340.
- [10] GAMBAUDO, J. M. *Perturbation of a Hopf bifurcation by an external time-periodic forcing*. J. Diff. Eqns. **57** (1985), pp. 172–199.
- [11] GERSHUNI, G. Z. & ZHUKHOVITSKII, E. M. *On parametric excitation of convective instability*. J. Applied Math. & Mech. **27** (1964), pp. 1197–1204.
- [12] GRESHO, P. M. & SANI, R. L. *The effects of gravity modulation on the stability of a heated fluid layer*. J. Fluid Mech. **40** (1970), pp. 783–806.
- [13] GUCKENHEIMER, J. & HOLMES, P. *Nonlinear Oscillations, Dynamical Systems, and Bifurcations of Vector Fields*, Springer–Verlag, 1986.
- [14] HU, H. C. & KELLY, R. E. *Effect of a time-periodic axial shear flow upon the onset of Taylor vortices*. Phys. Rev. E **51** (1995), pp. 3242–3251.
- [15] JORDAN, D. W. & SMITH, P. *Nonlinear Ordinary Differential Equations*, Oxford, 1977.
- [16] JOSEPH, D. D. *Stability of Fluid Motions I*, Springer–Verlag, 1976.
- [17] KATO, T. *Perturbation Theory for Linear Operators*, Springer–Verlag, 1966.
- [18] KELLY, R. E. *The stability of an unsteady Kelvin–Helmholtz flow*. J. Fluid Mech. **22** (1965), pp. 547–560.
- [19] KUZNETSOV, Y. A. *Elements of Applied Bifurcation Theory*, Springer–Verlag, 1995.
- [20] MARQUES, F. & LOPEZ, J. M. *Taylor–Couette flow with axial oscillations of the inner cylinder: Floquet analysis of the basic flow*. J. Fluid Mech. **348** (1997), pp. 153–175.
- [21] MATHIEU, E. *Mémoire sur le mouvement vibratoire d’une membrane de forme elliptique*. J. Math. **13** (1868), pp. 137–203.
- [22] MCKARNIN, M. A., SCHMIDT, L. D. & ARIS, R. *Forced oscillations of a self-oscillating bimolecular surface reaction model*. Proc. R. Soc. Lond. A **417** (1988), pp. 363–388.
- [23] MILES, J. & HENDERSON, D. M. *Parametrically forced surface waves*. Annu. Rev. Fluid Mech. **22** (1990), pp. 143–165.
- [24] PECKHAM, B. B. *The necessity of the Hopf bifurcation for periodically forced oscillators*. Nonlinearity **3** (1990), pp. 261–280.
- [25] PECKHAM, B. B., FROUZAKIS, C. E. & KEVREKIDIS, I. G. *Bananas and banana splits: a parametric degeneracy in the Hopf bifurcation for maps*. SIAM J. Math. Anal. **26** (1995), pp. 190–217.
- [26] WEISBERG, A. Y. *Control of transition in Taylor–Couette flow with axial motion of the inner cylinder*. Ph.D. Thesis, Princeton University, 1996.
- [27] WEISBERG, A. Y., KEVREKIDIS, I. G. & SMITS, A. J. *Delaying transition in Taylor–Couette flow with axial motion of the inner cylinder*. J. Fluid Mech. **348** (1997), pp. 141–151.